



16-Bromoepiandrosterone, an activator of the mammalian immune system, inhibits glucose 6-phosphate dehydrogenase from *Trypanosoma cruzi* and is toxic to these parasites grown in culture

Artur T. Cordeiro^{a,*}, Otavio H. Thiemann^b

^a Laboratório Nacional de Biotecnologia, Centro de Pesquisa em Energia e Materiais, R. Giuseppe Máximo Scolfaro, 10000 Campinas, Brazil

^b Centro de Biologia Molecular Estrutural, Instituto de Física de São Carlos, Universidade de São Paulo, Av. Trabalhador São Carlense 400, São Carlos, Brazil

ARTICLE INFO

Article history:

Received 12 March 2010

Revised 3 May 2010

Accepted 4 May 2010

Available online 7 May 2010

Keywords:

Epiandrosterone

Glucose-6-phosphate dehydrogenase

Trypanosoma cruzi

Chagas' disease

ABSTRACT

Glucose 6-phosphate dehydrogenase (G6PDH) catalyzes the first step of the pentose-phosphate pathway which supplies cells with ribose 5-phosphate (R5P) and NADPH. R5P is the precursor for the biosynthesis of nucleotides while NADPH is the cofactor of several dehydrogenases acting in a broad range of biosynthetic processes and in the maintenance of the cellular redox state. RNA interference-mediated reduction of G6PDH levels in bloodstream-form *Trypanosoma brucei* validated this enzyme as a drug target against Human African Trypanosomiasis. Dehydroepiandrosterone (DHEA), a human steroidal pro-hormone and its derivative 16 α -bromoepiandrosterone (16BrEA) are uncompetitive inhibitors of mammalian G6PDH. Such steroids are also known to enhance the immune response in a broad range of animal infection models. It is noteworthy that the administration of DHEA to rats infected by *Trypanosoma cruzi*, the causative agent of Human American Trypanosomiasis (also known as Chagas' disease), reduces blood parasite levels at both acute and chronic infection stages. In the present work, we investigated the in vitro effect of DHEA derivatives on the proliferation of *T. cruzi* epimastigotes and their inhibitory effect on a recombinant form of the parasite's G6PDH (TcG6PDH). Our results show that DHEA and its derivative epiandrosterone (EA) are uncompetitive inhibitors of TcG6PDH, with K_i values of 21.5 ± 0.5 and 4.8 ± 0.3 μ M, respectively. Results from quantitative inhibition assays indicate 16BrEA as a potent inhibitor of TcG6PDH with an IC_{50} of 86 ± 8 nM and those from in vitro cell viability assays confirm its toxicity for *T. cruzi* epimastigotes, with a LD_{50} of 12 ± 8 μ M. In summary, we demonstrated that, in addition to host immune response enhancement, 16BrEA has a direct effect on parasite viability, most likely as a consequence of TcG6PDH inhibition.

Crown Copyright © 2010 Published by Elsevier Ltd. All rights reserved.

1. Introduction

The pentose-phosphate pathway (PPP) converts glucose-phosphate to pentose-phosphates, essential precursors of nucleotides, and produces NADPH as reducing equivalents for biosynthetic processes and maintaining the redox balance. The pathway is organized in two parts, an irreversible oxidative decarboxylation of glucose 6-phosphate (G6P) to ribulose 5-phosphate (Ru5P) and a reversible non-oxidative interconversion of phosphorylated pentoses to glycolysis/gluconeogenesis intermediates (Fig. 1). Phosphoribosyl pyrophosphate (PRPP) formed from R5P is used in the biosynthesis of histidine and nucleotides. Alternatively to the PPP, most organisms have a ribokinase (EC 2.7.1.15) that allows cells to produce R5P by phosphorylation of internalized ribose units.¹ Moreover, NADPH might also be produced by different cytosolic enzymes, like malic enzyme (EC 1.1.1.40) or isocitrate dehydrogenase (EC 1.1.1.42).

Redundancy in pathways producing R5P and NADPH points to the importance of such metabolites to cellular viability. Although PPP might be dispensable for basal growth of mammalian cells under culture conditions, G6PDH-deleted mouse embryonic stem cells present a reduced cloning efficiency that can be reverted by reduction of the oxygen pressure in the medium.² In humans, G6PDH deficiency is a hereditary metabolic disorder which in the most severe cases results in hemolytic anemia, usually triggered by contact of red blood cells with oxidative agents.³ The NADPH produced by G6PDH and 6PGLDH is used by two opposing processes involved in the maintenance of the redox balance in mammalian cells. In phagocytosing cells, NADPH supplies electrons for the production of nitric oxide (NO) and reactive oxygen species (ROS), a process known as 'oxidative burst' that is catalyzed by the NADPH-dependent inducible NO synthase (EC 1.14.13.39) and NADPH-oxidase (EC 1.6.3.1).⁴ To control the oxidative burst and neutralize the excess of NO and ROS, cells rely on glutaredoxin and thioredoxin systems,⁵ where glutathione reductase (EC 1.8.1.7) and thioredoxin reductase (EC 1.8.1.9), both

* Corresponding author. Tel.: +55 19 35121121; fax: +55 19 35121006.

E-mail address: artur.cordeiro@cebime.org.br (A.T. Cordeiro).

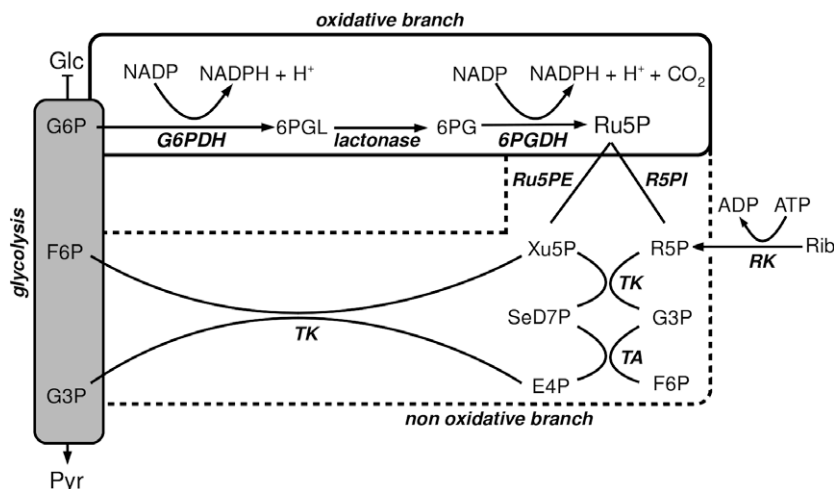


Figure 1. Overview of the pentose-phosphate pathway (PPP) and its connection to glycolysis. PPP begins with the oxidation of glucose 6-phosphate (G6P) to 6-phosphogluconolactone (6PGL) with concomitant reduction of NADP⁺ to NADPH, catalyzed by the glucose 6-phosphate dehydrogenase (**G6PDH**, EC 1.1.1.49). In the following two steps of the oxidative branch, lactonase (EC 3.1.1.31) catalyzes the hydrolysis of 6PGL to 6-phosphogluconate (6PG), and 6-phosphogluconate dehydrogenase (**6PGDH**, EC 1.1.1.44) promotes the oxidative decarboxylation of 6PG to ribulose-5-phosphate (Ru5P), with reduction of an additional NADP⁺ to NADPH. The PPP non-oxidative branch starts with the isomerization and epimerization of Ru5P to ribose 5-phosphate (R5P) and xylulose 5-phosphate (Xu5P), catalyzed by ribulose 5-phosphate epimerase (**Ru5PE**, EC 5.1.3.1) and ribose 5-phosphate isomerase (**R5PI**, EC 5.3.1.6), respectively. Then it proceeds through the alternated action of transketolase (**TK**, EC 2.2.1.1) and transaldolase (**TA**, EC 2.2.1.2) producing glyceraldehyde 3-phosphate (G3P) and fructose 6-phosphate (F6P). Alternatively to the PPP, most organisms have a ribokinase (**RK**, EC 2.7.1.15) that allows cells to produce R5P by phosphorylation of internalized ribose (Rib) units.

NADPH-dependent enzymes, play pivotal roles. Parasites belonging to the protist Trypanosomatidae family, which includes *Trypanosoma brucei*, *Trypanosoma cruzi* and *Leishmania* spp. also rely on PPP to supply their oxidative defence system with reducing equivalents. Nevertheless, trypanosomatids lack thioredoxin reductase and instead of glutathione its thiol redox component is the trypanothione (N¹,N⁸-bis-glutathionyl-spermidine). The NADPH-dependent trypanothione reductase is exclusively found in trypanosomatids and is essential for parasite proliferation and neutralization of the host oxidative burst.⁶

T. cruzi is the causative agent of Chagas' disease, which is estimated to affect 18 million people in American tropical and subtropical areas. Chagas' disease progresses from an early and often asymptomatic acute phase to a chronic and usually symptomatic disease. One third of the people living with chronic Chagas' disease are expected to develop heart insufficiency and half of them are not expected to live more than two years after the onset of cardiac complication symptoms.⁷ There is no effective treatment for Chagas' disease. The available anti-trypanosome drugs, Nifurtimox and Benznidazole are highly toxic to mammalian cells and consequently provoke undesired side effects. Their mechanism of action is not precisely understood, but both drugs are known to release reactive nitrogen species that kill the parasites but are also toxic to the mammalian host cells.⁸

T. cruzi G6PDH (TcG6PDH) was demonstrated to play a prominent role for parasite survival when submitted to oxidative stress conditions.⁹ In *T. brucei* bloodstream forms, the RNA interference (RNAi)-mediated reduction of G6PDH levels affected normal cell proliferation, killing parasites within 48 h after induction of the enzyme's depletion.¹⁰ Additionally, it was shown for the first time that the pro-hormone dehydroepiandrosterone (DHEA) is also able to inhibit non-mammalian G6PDHs by an uncompetitive mechanism identical to that observed for human G6PDH¹¹ and, in the case of TbG6PDH, with an inhibition constant in the low micromolar range. Moreover, in vitro growth of bloodstream-form *T. brucei* was interrupted by the addition of DHEA to the medium. Together, these data provided both a genetic and chemical validation of TbG6PDH as target for the development of new drugs against Human African Trypanosomiasis. In the work presented here, we (1) describe the kinetic mechanism of TcG6PDH; (2) the mechanism

through which it is inhibited by DHEA and EA; (3) evaluate, by a quantitative assay, the effect of DHEA, Epiandrosterone (EA), 16- α -bromo-dehydroepiandrosterone (16BrDHEA) and 16- α -bromo-epiandrosterone (16BrEA) on TcG6PDH activity; and (4) determine the effect of these steroids on the in vitro growth of *T. cruzi* epimastigotes (i.e., the form of the parasite present in the insect vector).

2. Results

2.1. *T. cruzi* G6PDH purification and kinetic mechanism

N-Terminally His-tagged TcG6PDH was expressed in *Escherichia coli* BL21 transformed with recombinant pET28 plasmids containing the gene encoding the long form of the enzyme, and purified to homogeneity by a single nickel affinity chromatographic step. Approximately 5 mg of pure TcG6PDH were recovered per liter of *E. coli* culture. Enzyme kinetic analyses were performed with His-tagged TcG6PDH. Reaction velocities, expressed as nmoles of NADPH produced per second, were obtained by varying the G6P concentration at different concentrations of NADP⁺. The convergence of Lineweaver-Burk lines (Fig. 2) is consistent with a sequential mechanism.¹² Linear fit of secondary plots ($1/V_{\text{app}}^{\text{G6P}}$ vs $1/[\text{NADP}^+]$ and $(K_m/V_{\text{max}})^{\text{app-G6P}}$ versus $1/[\text{NADP}^+]$) allowed the calculation of kinetic constants using Cleland's velocity equation:

$$v = V_1[A][B]/(K_{ia}K_b + K_b[A] + K_a[B] + [A][B]),$$

where K_a and K_b are the Michaelis constants for substrates A (G6P) and B (NADP⁺), respectively; and V_1 and K_{ia} are the maximum velocity and a constant, respectively. The kinetic constants derived for TcG6PDH are shown in Table 1.

2.2. Inhibition mechanism of *T. cruzi* G6PDH by steroids

TcG6PDH is uncompetitively inhibited by DHEA and EA. For enzymes with a sequential mechanism, the uncompetitive inhibition is distinguishable from a competitive mechanism due to proportional changes in apparent K_m and V_{max} values, calculated from data obtained in assays with enzyme in the presence of different inhibitor concentrations. Uncompetitive inhibitors can be readily identified by inspection of Lineweaver-Burk plots, in which proportional

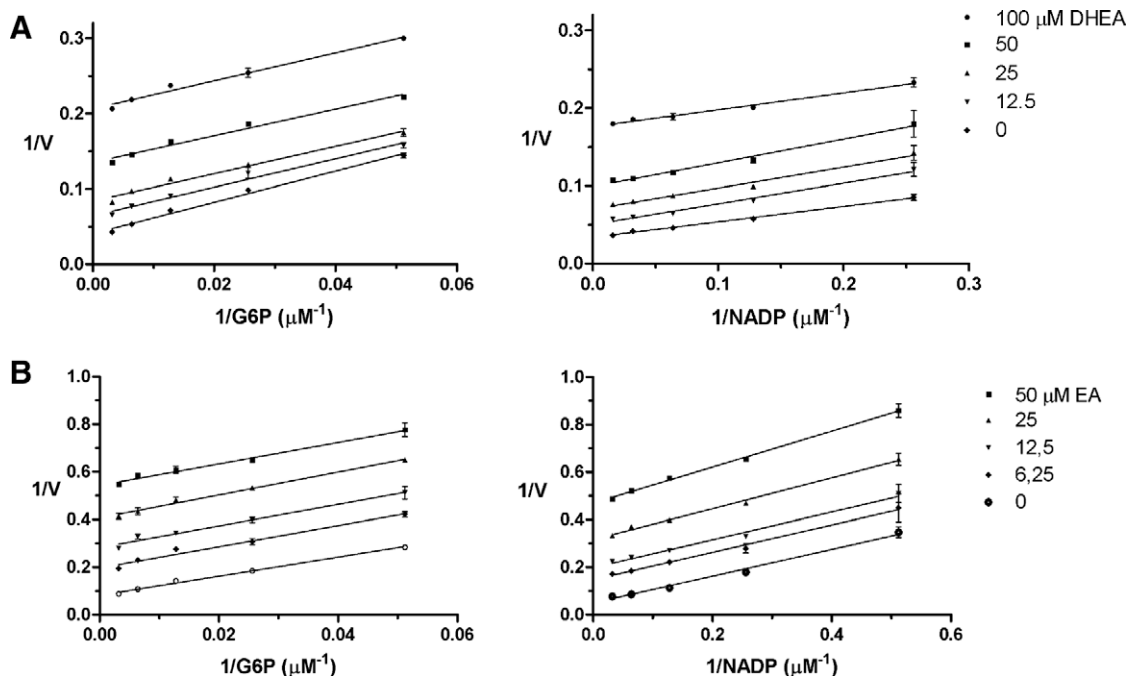


Figure 2. (A) Dehydroepiandrosterone (DHEA) and (B) epiandrosterone (EA) inhibition of *T. cruzi* G6PDH. Inhibitors were assayed against each substrate in separate experiments. First, G6P was varied from 1250 to 9.77 μM with NADP⁺ fixed at a saturating concentration (250 μM), then NADP⁺ was varied from 250 to 1.95 μM while G6P was kept at a saturating concentration (1.25 mM). The parallel lines in the Lineweaver-Burk plots confirm that DHEA and EA are uncompetitive inhibitors of TcG6PDH.

Table 1
Kinetic and inhibition constants of recombinant *T. cruzi* G6PDH

<i>T. cruzi</i> G6PDH		
<i>Kinetic constants</i>		
Mechanism	Sequential	
K_{G6P} (μM)	206.0 ± 4.2	
K_{NADP} (μM)	22.5 ± 1.2	
V_1 (nmoles of NADPH s ⁻¹)	77.7 ± 2.5	
k_{cat} (s ⁻¹)	57.1 ± 1.9	
K_{IG6P} (μM)	105.3 ± 4.6	
<i>Inhibition constants</i>		
Mechanism	Uncompetitive	
	G6P	NADP
K'_i _DHEA (μM)	21.5 ± 0.5	22.3 ± 0.5
K'_i _EA (μM)	4.8 ± 0.3	4.8 ± 0.3

changes of apparent K_m and V_{max} result in a family of parallel lines (Fig. 3). DHEA and EA K_i values were independently calculated for both TcG6PDH substrates and are reported in Table 1.

2.3. Quantitative TcG6PDH inhibition by DHEA derivatives

In the established quantitative G6PDH inhibition assay, the effect of different concentrations of inhibitors, varying from 0.0048 to 40 μM , was measured at fixed concentrations of the substrates for the forward reaction (G6P and NADP⁺). IC₅₀ values for DHEA, EA, 16BrDHEA, and 16BrEA corresponding to the inhibitor concentrations that reduce the reaction velocity by 50%, were calculated from the respective dose-response curves (Fig. 4) and are shown in Table 2.

2.4. In vitro toxicity assays of DHEA derivatives against cultured *T. cruzi* epimastigotes

The reduction of 3-(4,5-dimethylthiazol-2-yl)-5-(3-carboxymethoxyphenyl)-2-(4-sulphophenyl)-2H-tetrazolium, inner salt (MTS) to formazan was used as a measure of viable cells grown

in the presence of different concentrations of DHEA, EA, 16BrDHEA, and 16BrEA. LD₅₀ values, corresponding to the concentration of each compound that reduces the number of viable cells by 50%, were calculated from dose-response fitted curves (Fig. 5) and are shown in Table 2.

3. Discussion

3.1. *T. cruzi* G6PDH as metabolic target for DHEA derivatives

The characterization of the TcG6PDH enzymatic mechanism indicates that it follows a sequential mechanism (Fig. 2), in which a ternary complex is established between the enzyme and both substrates, G6P and NADP⁺. Such a ternary complex is required for binding of uncompetitive inhibitors, like we demonstrated here to be the case for DHEA and EA, against both substrates (Fig. 3). True uncompetitive inhibition of a bireactant system is relatively unusual. Frequently, an inhibitor may be uncompetitive with respect to one substrate, but competitive to the other substrate. Although rarely found in metabolism, true uncompetitive inhibition is claimed as the better choice for the discovery of more effective drugs and pesticides. That is because the effect of a competitive inhibitor in a metabolic pathway can be reversed by the accumulation of substrates of the targeted enzyme, while in the case of an uncompetitive inhibitor the blockage can only be overcome by the increase of the enzyme to inhibitor ratio¹³ and consequently it would be necessary to increase the enzyme expression level. The metabolic effect of an uncompetitive inhibitor, either the substrate accumulation or the product depletion, might compromise the viability of a living organism before the cells may be able to raise an effective response. Inhibition of TcG6PDH will cause a reduction in the parasite's cytosolic NADPH content. With reduced NADPH levels, several biosynthetic processes necessary for normal parasite growth might be affected. Since its trypanothione system will also be indirectly affected by the reduced NADPH production, the parasite might become more susceptible to the

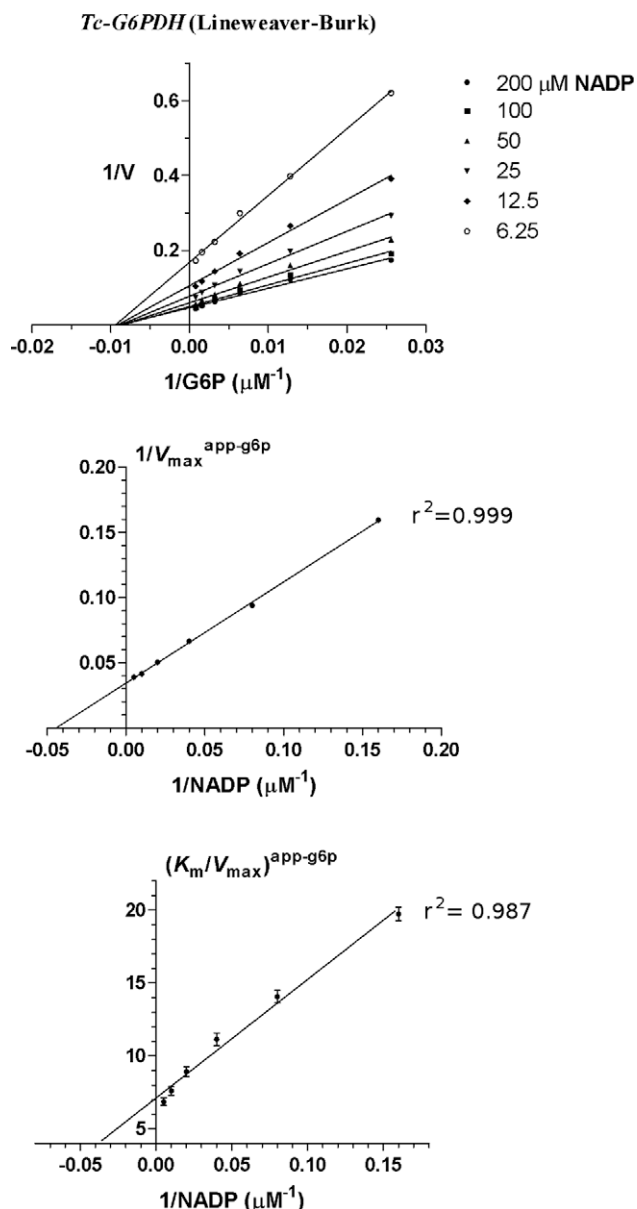


Figure 3. Lineweaver-Burk and secondary plots for TcG6PDH. Velocity (V) is expressed in nmoles of NADPH produced per second. In Lineweaver-Burk plots, each curve was obtained at a fixed concentration of NADP⁺ (as indicated aside of the plots) while the G6P concentration was varied from 1250 to 39 μM (resulted of a twofold serial dilution).

oxygen pressure of its environment. In this respect it is noteworthy that in *T. brucei* the conditional knockout of trypanothione reductase arrested in vitro parasite growth, increased its susceptibility to hydrogen peroxide and reduced its virulence.¹⁴

In general, a criterion used to select a promising target against infectious diseases is the absence of a host homologous molecule, or a homologue that is very different. Pairwise sequence alignments (data not shown) among *T. cruzi*, *T. brucei*, and *L. mexicana* G6PDHs returned values around 62% of amino-acid identity. These values drop to 48% when trypanosomatid enzymes are compared to human G6PDH. Due to the uncompetitive inhibition mechanism, planarity, and hydrophobicity, DHEA should bind to a hydrophobic tight caveat present exclusively in the enzyme-substrates complex. Visual inspection of human G6PDH crystallographic structures superposed with TcG6PDH homology based model does not provide insights into the location of the putative DHEA binding caveat. The characterization of the DHEA binding site will allow

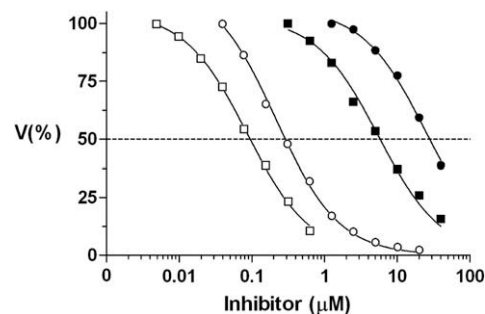


Figure 4. Quantitative inhibition of *T. cruzi* G6PDH activity by DHEA (filled circle), EA (filled square), 16BrDHEA (open circle), and 16BrEA (open square). Data for each compound were adjusted to a dose-response curve. IC₅₀ values, corresponding to inhibitor concentrations that reduce the reaction velocity by 50%, were retrieved from the curves shown in this figure and are given in Table 2.

chemistries to explore structural differences between the human and trypanosomatid G6PDHs to produce selective inhibitors against the parasite enzyme. Even if DHEA derivatives designed to target the TcG6PDH present a residual inhibitory effect on the human homologous enzyme, it is worth noting that humans can live with reduced G6PDH levels, as observed in people with a mild to moderate G6PDH deficiency due to a genetic disorder. Indeed, it has been demonstrated that G6PDH-deleted mammalian stem cells can grow in usual Dulbecco's Modified Eagle's medium, but display an impaired cloning efficiency.² In unmodified stem cells, isocitrate dehydrogenase and malic enzyme also contribute to the cytosolic production of NADPH, but only G6PDH is overexpressed in response to oxidative stress conditions.¹⁵ Together these findings suggest that TcG6PDH can be considered a promising target for the design of modern drugs against Chagas' disease.

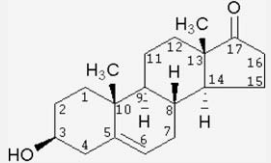
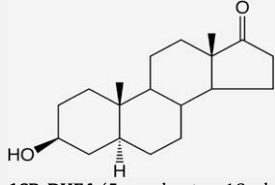
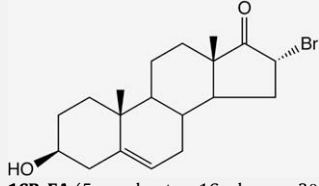
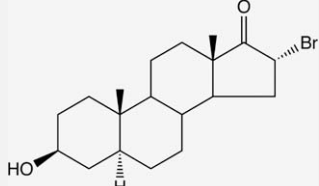
3.2. In vitro toxicity of DHEA derivatives to *T. cruzi* epimastigotes

According to Igoillo-Esteve and coauthors, among the four life forms of *T. cruzi*, the epimastigote presents the lowest G6PDH levels, most probably because inside the insect's digestive tract the parasite is not exposed to an oxidative environment and consequently, it seems logical not to need an elaborate oxidative defense system. The susceptibility of *T. cruzi* epimastigotes to DHEA derivatives, like EA, 16BrDHEA, and 16BrEA, suggests that even in the absence of oxidative agents the parasite requires a basal G6PDH activity to sustain normal growth. That was also observed for *T. brucei* bloodstream forms cultured in the presence of DHEA or EA at non-oxidative conditions.¹⁰ Although, recombinant TcG6PDH is uncompetitively inhibited by DHEA, we could not detect a relevant toxic effect of DHEA against *T. cruzi* epimastigotes. Probably, the intracellular DHEA concentration is lower than the extracellular one, perhaps explained by a possible enzymatic conversion of DHEA into androstenediol and androstenedione,¹⁶ which are known to have no effect on human G6PDH activity.¹⁷ Modification of the DHEA formula, by halogenation of position C-16 provided 16 α -fluor-epian-drosterone¹⁸ and 16BrEA^{19,20} which are better inhibitors of human G6PDH and are not converted to androgens. EA, 16BrDHEA, and 16BrEA were here demonstrated to be better inhibitors of TcG6PDH than DHEA. Indeed, they are also toxic to *T. cruzi* epimastigotes, with LD₅₀ values in the low micromolar range (Table 2).

3.3. DHEA interaction with immune system and parasite toxicity in different infectious diseases

DHEA and DHEA-sulfate (DHEAS) are inactive precursor steroids synthesized from cholesterol in adrenal glands and further converted into potent androgens and estrogens in peripheral tis-

Table 2Quantitative inhibition (IC_{50}) of *T. cruzi* G6PDH and toxicity for cultured epimastigotes (LD_{50}) by DHEA and derivatives

No.	Compound	IC_{50} (μ M)	LD_{50} (μ M)
1	DHEA (5 α -androst-3 β -ol-17-one)  EA (5 α -androstan-3 β -ol-17-one)	25.0 ± 3.5	nd ^a
2	 16BrDHEA (5 α -androst-16 α -bromo-3 β -ol-17-one)	5.6 ± 1.2	36.5 ± 3.6
3	 16BrEA (5 α -androstan-16 α -bromo-3 β -ol-17-one)	0.216 ± 0.024	20.6 ± 2.2
4	 16BrEA (5 α -androstan-16 α -bromo-3 β -ol-17-one)	0.086 ± 0.008	12.4 ± 1.2

95% confidence interval.

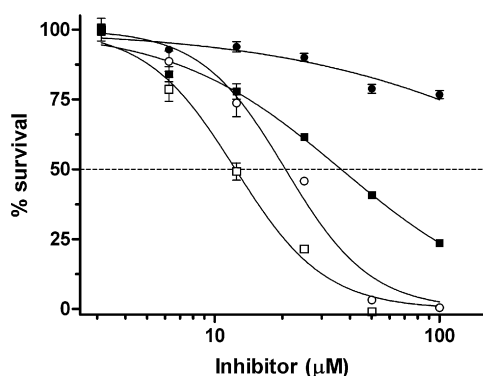
^a nd, not detected within the inhibitor concentration range assayed.

Figure 5. *T. cruzi* epimastigote viability at different concentrations of DHEA (filled circle), EA (filled square), 16BrDHEA (open circle), and 16BrEA (open square). Data for each compound were adjusted to a dose-response curve. LD_{50} values, corresponding to inhibitor concentrations that reduces the viable cells by 50%, were retrieved from the curves shown in this figure and are given in Table 2.

sues.²¹ DHEA and DHEAS secretion declines with age resulting in the reduction of circulating androgen and estrogen hormones. Although inactive as a hormone, DHEA is a potent inhibitor of mammalian G6PDH, without activity on yeast or plant homologous enzymes.²² G6PDH inhibition by DHEA lowers cytoplasmic levels of NADPH and reduces the NADPH-dependent free radicals production. The effective control of the oxidative burst during inflammatory processes plays an important role in prevention of autoimmune diseases, cancer²³ and the general aging process.²⁴

In adipocytes, the adenovirus mediated overexpression of G6PDH leads to expression of pro-oxidative enzymes and inflammatory cytokines associated with several obesity-mediated diseases like insulin resistance, type-2 diabetes and arteriosclerosis.²⁵ In such cells, it was found that G6PDH inhibition by DHEA leads to reduction of expression of pro-oxidative enzymes, like iNOS and NADPH-oxidase, and inflammatory cytokines like tumor necrosis factor alpha (TNF- α) and interleukine-6 (IL-6). Together, these data suggest that control of G6PDH activity might protect mammalian cells from an exacerbated immune reaction.

In addition to controlling the inflammatory process, DHEA and 16BrEA have been demonstrated to reduce parasitemia in animal models for different infectious diseases and to impair parasite viability in in vitro experiments (Table 3). The available data can be arranged in two distinct groups, one that suggests DHEA to act as a modulator of the host immune response^{26–31} and another that demonstrates its toxic effect on cultured parasites.^{10,27,32–35} DHEA efficacy on the immune system is supported by the increase of cytokine levels associated with a type-1 immune response, triggered by infection with *Mycobacterium tuberculosis*²⁸ and *T. cruzi*.^{29–31} Contrary to these findings, prophylactic DHEA administration to mice causes a reduction in *Taenia crassiceps* load without altering Th1 cytokine levels.³⁵ These conflicting data show that one has to be prudent in generalizing the DHEA immune modulation properties to all infectious diseases and in assuming that the enhancement of the host immunity is the unique cause of parasitemia reduction and disease control. In vitro DHEA toxicity has been demonstrated against parasites from distinct phylogenetic branches, like protozoa^{10,27} (*Trypanosoma*, *Plasmodium*) and meta-

Table 3

Examples of the efficacy of DHEA (and its derivatives) in the treatment of bacterial, protozoan, and metazoan infectious diseases

Parasite	Experimental measure	Action mechanism (<i>experimental evidence</i>)	Ref.
<i>Active through the host immune response modulation</i>			
<i>Cryptosporidium parvum</i>	– Fecal oocyst shedding – Parasite colonization in mouse intestine	Unclear	26
<i>Plasmodium berghei</i>	– Parasitemia of infected rats treated with 16BrEA	Unclear	27
<i>Mycobacterium tuberculosis</i>	– Number of colony-forming units in lungs of infected mice treated with 16BrEA – Effect of 16BrEA on expression of iNOS, IFN- γ , TNF- α , IL-2, and IL-4	Enhancement of Th1 immune response (increased levels of IFN- γ , TNF- α and iNOS)	28
<i>Trypanosoma cruzi</i>	– Parasitemia of infected rats – IFN- γ , IL-2 levels – Parasitemia of infected rats during acute and chronic infection stages – IL-12 and NO levels – Parasitemia of infected rats – TNF- α and NO levels – In vitro parasite growth inhibition	Enhancement of Th1 immune response (increased levels of IFN- γ and IL-2) Enhancement of Th1 immune response at both stages (increased levels of IL-12 and NO) – Enhancement of Th1 immune response (increased levels of TNF- α and NO) – Low parasite toxicity ($LD_{50}^{DHEA} = 1064 \mu M$)	29 30 31
<i>Parasite toxicity independent of host immune system</i>			
<i>P. falciparum</i>	In vitro parasite growth	Plasmodial cytotoxicity ($LD_{50}^{16BrEA} = 7.5 \mu M$)	27
<i>Schistosoma mansoni</i>	In vitro assessment of parasite viability and oviposition	Reduction of parasite viability and oviposition	32
<i>P. berghei</i> (CQ resistant)	– DHEAS effect on parasitemia in mice – Intra parasite GSH level and G6PDH activity	G6PDH inhibition and reduction of GSH levels	33
<i>Entamoeba histolytica</i>	– In vitro parasite growth – Measurement of DNA synthesis and putative G6PDH and HMGR activities in parasites extracts	HMGR inhibition ($IC_{50}^{DHEA} = 89 \mu M$)	34
<i>Taenia crassiceps</i>	– In vivo parasite growth and reproduction – Measure of IL-2, IL-4, IL-10 or IFN- γ mRNA levels from treated mice – In vitro parasite growth	In vivo protection to parasite infection and in vitro parasite growth inhibition, without alteration on cytokine levels	35
<i>T. brucei</i>	– In vitro parasite growth – RNAi-mediated reduction of G6PDH expression – Inhibition of recombinant TbG6PDH by DHEA	– In vitro parasite toxicity ($LD_{50}^{DHEA} = 43.8 \mu M$) – TbG6PDH inhibition ($K_i^{DHEA} = 1.7 \mu M$)	10
<i>T. cruzi</i>	– In vitro parasite growth – Inhibition of recombinant TcG6PDH	– In vitro parasite toxicity ($LD_{50}^{16BrEA} = 12 \mu M$) – TcG6PDH inhibition ($K_i^{16BrEA} = 0.08 \mu M$)	Present work

zoa^{32,35} (*Schistosoma* and *Taenia*). Such parasites will grow in different host environments, with different nutritional resources and, consequently, will depend on different metabolic routes. It would be rather unlikely to identify a common metabolic target for DHEA in all these parasites. In fact, two metabolic targets were already identified in different parasites. In the bloodstream form of *T. brucei*, the RNAi-mediated reduction of G6PDH levels impaired parasite growth. The recombinant *T. brucei* G6PDH was inhibited by DHEA and EA, and both compounds were toxic to the parasites cultured in vitro.¹⁰ In *Entamoeba histolytica*, which lacks the oxidative branch of the PPP, DHEA inhibited a putative hydroxymethylglutaryl-CoA reductase (HMGR) activity, which is a key enzyme for the biosynthesis of isoprenes.³⁴ Based on the reviewed data, we suggest that the in vivo DHEA efficacy in treatment of infectious diseases might often be a combination of modulation of the host immune response with a direct toxicity to the infectious agent, through interference with its metabolism. Indeed, to support any DHEA anti-parasite therapy, its effect on both the host immunity and parasite viability should be independently evaluated.

4. Conclusion

In the presented work, It is shown that TcG6PDH is uncompetitively inhibited by DHEA and EA. A quantitative assay confirmed that halogenification of DHEA (and EA) at position 16 resulted in better TcG6PDH inhibitors; with IC_{50} values for 16BrEA below 100 nM. In vitro parasite viability assays showed that DHEA derivatives, like EA, 16BrDHEA, and 16BrEA are toxic to *T. cruzi* epimastigotes. Although DHEA inhibits recombinant TcG6PDH, it does not have a detectable toxic effect on parasite viability below the highest tested concentration (100 μM). The parasite tolerance to

DHEA might be consequence of its conversion to androstenediol and androstenedione.¹⁶ Despite the stimulation of the immune system, DHEA derivatives were toxic to a broad range of parasites in in vitro experiments. Our data support the inclusion of *T. cruzi* in the list of parasites susceptible to DHEA derivatives and necessitates the investigation of the TcG6PDH–DHEA complex structure for its use in the development of new drugs against Chagas' disease.

5. Experimental

5.1. TcG6PDH expression, purification, and steady-state kinetics

The cloning of the TcG6PDH gene in the pET28 expression vector has been described elsewhere.⁹ TcG6PDH was overexpressed in *E. coli* BL21 transformed with the recombinant pET28 constructs and incubated in ZYM-5052 autoinduction medium for 48 h at 25 °C. Cells were harvested by centrifugation at 4000 g during 20 min and disrupted in a French press cell at 13,000 psi. His-tagged TcG6PDH was purified to homogeneity by metal affinity chromatography on columns containing 4 ml Ni-NTA resin (Invitrogen) following the manufacturer's recommended procedure. TcG6PDH was eluted with 50 mM triethanolamine pH 7.6 and 0.4 M imidazole. In order to determine the reaction mechanism of TcG6PDHs, the rates of NADPH formation were measured at 340 nm in a SpectraMax Plus³⁸⁴ spectrophotometer (Molecular Devices), using a 96 well titer plate and a final reaction volume of 0.2 ml per well. All pipetting steps were performed automatically in a Biomek3000 robot (Beckman Coulter). Initially, 5 μl of different G6P stock solutions were loaded into wells of the first four columns. The reaction was started simultaneously in all wells of each

column by addition of a solution mixture containing the enzyme (1.4 nM TcG6PDH) and NADP⁺ (200, 100, 50, 25, 12.5, and 6.25 μM) in RB reaction buffer (50 mM triethanolamine pH 7.6, 2.5 mM MgCl₂). The robot took less than 20 s to load solutions into the four columns of the plate. The concentration of TcG6PDH in the solution mixture was chosen in order to allow the measurement of constant NADPH formation rates for a minimum of 60 s. In wells in each plate's row, the reaction occurs at different G6P ranging from 1250 to 39 μM (resulted of a twofold serial dilution) and a unique NADP⁺ concentration. The procedure was repeated for the different NADP⁺ concentrations. The $K_m^{app-G6P}$ and $V_{max}^{app-G6P}$ for different NADP⁺ concentrations were calculated from Lineweaver–Burk plots. In '1/V^{app-G6P}_{max} versus 1/NADP⁺' secondary plots, the y-intercept (when x = 0) and x-intercept (when y = 0) correspond to 1/V₁ and -1/K_{NADP}, respectively; and in '(K_m/V_{max})^{app-G6P} versus 1/NADP⁺' secondary plots, the y-intercept (when x = 0) and x-intercept (when y = 0) correspond to K_{G6P}/V₁ and -K_{G6P}/(K_{NADP} · K_{IG6P}), respectively. The parameters V₁, K_{G6P}, K_{NADP}, and K_{IG6P} are the kinetic constants from Cleland's¹⁸ equation.

5.2. DHEA and EA inhibition mechanism

Twenty-fold DHEA and EA stock solutions were prepared in 50% DMSO. In the final reaction volume, the DMSO concentration was reduced to 2.5%, which had no effect on TcG6PDH activity. TcG6PDH was assayed in the presence of concentrations of EA varying between 50 and 6.25 μM and DHEA between 100 and 12.5 μM of DHEA. A Biomek3000 robot was used to pipette assay solutions into 96 well plates and NADPH formation rates were recorded in SpectraMax Plus³⁸⁴ (Molecular Devices). The final reaction volume was 0.2 ml per well. TcG6PDH inhibition was assayed separately for G6P and NADP⁺. For G6P as varying substrate, 5 μl of G6P stock solutions were loaded into wells of four plate's columns, each plate row received a different G6P concentration varying from 1250 to 9.77 μM. The reaction was initiated by addition of a solution mixture containing the enzyme (1.4 nM), inhibitor and NADP⁺ (0.25 mM) in RB reaction buffer. For NADP⁺ as varying substrate, 5 μl of NADP⁺ stock solutions were loaded into wells of four plate's columns, each plate row received a different NADP⁺ solution. The final NADP⁺ concentration varied from 250 to 1.95 μM. The reaction was initiated by addition of a solution mixture containing the enzyme (2 nM), inhibitor and G6P (1.25 mM) in RB reaction buffer. Linear absorbance rates were recorded for 80 s.

5.3. Quantitative inhibition assays

Each tested compound was initially prepared at 4 mM in 100% DMSO. Stock solutions were obtained applying a 50% serial dilution in 100% DMSO. Five microliters of each inhibitor stock solution were placed in the bottom of a 0.5 ml quartz cuvette. Next, 245 μl of RB containing 0.4 mM NADP and 2 mM G6P was added to each cuvette. The reaction was started by addition of 250 μl RB containing TcG6PDH (4 nM). The NADPH production rates from six different cuvettes were measured simultaneously at 340 nm in a Cary100Bio spectrophotometer (Varian). Data obtained from three independent experiments were normalized and fitted to a sigmoidal curve.

5.4. T. cruzi viability assay

2 × 10⁶ cells of *T. cruzi* (Y strain) epimastigotes were incubated in 1 ml LIT medium with 1% DMSO and DHEA, EA, 16BrDHEA or 16BrEA at concentrations of 3.12, 6.25, 12.5, 25, 50, and 100 μM for 72 h at 28 °C. Next, 80 μl of MTS (5% PMS) from the CellTiter96[®]

AQ_{ueous} One Solution Cell Proliferation Assay (Promega) was added to 400 μl of each *T. cruzi* culture; the suspensions were distributed over a 96 well plate (100 μl per well) and incubated at 28 °C for an additional 3 h. Soluble formazan, produced by viable cells by reduction of MTS, was measured at 490 nm in a Cary50 microplate reader (Varian). Data obtained from three independent experiments were normalized and fitted to a sigmoidal curve.

Acknowledgments

A.T.C. acknowledges a current postdoctoral fellowship from the Fundação de Amparo a Pesquisa do Estado de São Paulo (FAPESP, contract no. 2007/02663-6). This research was supported by grants from the Center for Structural Molecular Biotechnology (CEPID-FAPESP contract no. 98/14138-2, to O.H.T.), and the São Paulo State Bioprospecting Network (FAPESP contract no. 05/51966-6, to O.H.T.). Both authors acknowledge Professor Paul Michels from the Research Unit for Tropical Diseases, de Duve Institute, Brussels, for critical review of this manuscript.

References and notes

- Park, J.; van Koeveerden, P.; Singh, B.; Gupta, R. S. *FEBS Lett.* **2007**, *581*, 3211.
- Pandolfi, P. P.; Sonati, F.; Rivi, R.; Mason, P.; Grosveld, F.; Luzzatto, L. *EMBO J.* **1995**, *14*, 5215.
- Cappellini, M. D.; Fiorelli, G. *Lancet* **2008**, *317*, 64.
- Babior, B. M. *Am. J. Med.* **2000**, *109*, 33.
- Holmgren, A. J. *Biol. Chem.* **1989**, *264*, 13963.
- Krauth-Siegel, R. L.; Comini, M. A. *Biochim. Biophys. Acta* **2008**, *1780*, 1236.
- Teixeira, A. R. L.; Nitz, N.; Guimaro, M. C.; Gomes, C.; Santos-Buch, C. A. *Postgrad. Med. J.* **2006**, *82*, 788.
- Maya, J. D.; Cassels, B. K.; Iturriaga-Vásquez, P.; Ferreira, J.; Faúndez, M.; Galanti, N.; Ferreira, A.; Morello, A. *Comp. Biochem. Physiol.* **2007**, *146*, 601.
- Igoillo-Esteve, M.; Cazzulo, J. J. *Mol. Biochem. Parasitol.* **2006**, *149*, 170.
- Cordeiro, A. T.; Thiemann, O. H.; Michels, P. A. M. *Bioorg. Med. Chem.* **2009**, *17*, 2483.
- Gordon, G.; Mackow, M. C.; Levy, H. R. *Arch. Biochem. Biophys.* **1995**, *318*, 25.
- Cleland, W. W. *Biochim. Biophys. Acta* **1963**, *67*, 104.
- Cornish-Bowden, A. F. E. B. S. *Lett.* **1986**, *203*, 3.
- Krieger, S.; Schwarz, W.; Ariyanayagam, M. R.; Fairlamb, A. H.; Krauth-Siegel, R. L.; Clayton, C. *Mol. Microbio.* **2000**, *35*, 542.
- Fisola, S.; Fico, A.; Pagliarunga, F.; Balestrieri, M.; Crooke, A.; Verde, P.; Abrescia, P.; Bautista, J. M.; Martini, G. *Biochem. J.* **2003**, *370*, 935.
- Vacchina, P.; Valdéz, R. A.; Gómez, Y.; Revelli, S.; Romano, M. C. *J. Ster. Biochem. Mol. Biol.* **2008**, *111*, 282.
- Raineri, R.; Levy, H. R. *Biochemistry* **1970**, *9*, 2233.
- Schwartz, A. G.; Lewbart, M. L.; Pashko, L. L. *Cancer Res.* **1988**, *48*, 4817.
- Glazier, E. R. *J. Org. Chem.* **1962**, *27*, 2937.
- Henderson, E.; Schwartz, A.; Pashko, L.; Abou-Gharbia, M.; Swern, D. *Carcinogenesis* **1981**, *2*, 683.
- Labrie, F.; Luu-The, V.; Bélanger, A.; Lin, S.-X.; Simard, J.; Pelletier, G.; Labrie, C. *J. Endocr.* **2005**, *187*, 169.
- Marks, P.; Banks, J. *Proc. Nat. Acad. Sci. U.S.A.* **1960**, *46*, 447.
- Bartsch, H.; Nair, J. *Langenbecks Arch. Surg.* **2006**, *391*, 499.
- Schwartz, A. G.; Pashko, L. L. *Ageing Res. Rev.* **2004**, *3*, 171.
- Park, J.; Choe, S.; Choi, A. H.; Kim, K. H.; Yoon, M. J.; Suganami, T.; Ogawa, Y.; Kim, J. B. *Diabetes* **2006**, *55*, 2939.
- Rasmussen, K. R.; Healey, M. C. *Antimicrob. Agents Chemother.* **1992**, *36*, 220.
- Freilich, D.; Ferris, S.; Wallace, M.; Leach, L.; Kallen, A.; Frincke, J.; Ahlem, C.; Hacker, M.; Nelson, D.; Herbet, J. *Am. J. Trop. Med. Hyg.* **2000**, *63*, 280.
- Hernández-Pando, R.; Aguilar-Leon, D.; Orozco, H.; Serrano, A.; Ahlem, C.; Trauger, R.; Schramm, B.; Reading, C.; Frincke, J.; Rook, G. A. W. *J. Infect. Dis.* **2005**, *191*, 299.
- Santos, C. D.; Toldo, M. P. A.; Santello, F. H.; Filipin, M. D. V.; Brazão, V.; do Prado, J. C., Jr. *Vet. Parasitol.* **2008**, *153*, 238.
- Caetano, L. C.; Santello, F. H.; Filipin, M. D. V.; Brazão, V.; Caetano, L. N.; Toldo, M. P. A.; Caldeira, J. C.; do Prado, J. C., Jr. *Vet. Parasitol.* **2009**, *163*, 27.
- Kuehn, C. C.; Oliveira, L. G. R.; Santos, C. R.; Ferreira, D. S.; Toldo, M. P. A.; de Albuquerque, S.; do Prado, J. C., Jr. *J. Pineal Res.* **2009**, *47*, 253.
- Morales-Montor, J.; Mitchell, R.; DeWay, K.; Hallal-Calleros, C.; Baig, S.; Damian, R. T. *J. Immunol.* **2001**, *167*, 4527.
- Safeukui, I.; Mangou, F.; Malvy, D.; Vincendeau, P.; Massalay, D.; Haumont, G.; Vatan, R.; Oliaro, P.; Millet, P. *Biochem. Pharmacol.* **2004**, *68*, 1903.
- Carrero, J. C.; Cervantes, C.; Moreno-Mendoza, N.; Saavedra, E.; Morales-Montor, J.; Laclette, J. *Microbes Infect.* **2006**, *8*, 323.
- Vargas-Villavicencio, J. A.; Larralde, C.; Morales-Montor, J. *Int. J. Parasitol.* **2008**, *38*, 775.